

ON A DESCRIPTION OF A NEW "HARDNESS" TEST

J. ZARKA and J. FRELAT

Laboratoire de Mécanique des Solides, Ecole Polytechnique Ecole Nationale Supérieure des Mines de Paris,
Equipe de Recherche associée C.N.R.S., 91120 Palaiseau, France

(Received 7 May 1976; revised 12 October 1976)

Abstract—It is shown that, if a structure is elastically homogeneous and if there is no residual stress, the elastic limit at any point of this structure may be easily measured by a non-destructive method thanks to a new kind of "hardness" test and a new automatic set-up.

1. INTRODUCTION

In order to optimize a structure, it is necessary to know its mechanical properties (constitutive relations) and the residual stresses in any point (which may be introduced during the working or the heat treatment). Indeed, the stress field which results from the residual stresses and the service stresses has to satisfy the yield criteria (for example the elastic limit or the fatigue limit. . .). However this knowledge of the mechanical properties and the residual stresses must result from non-destructive tests if we want to use the structure thereafter. The classical processes, which allow us to measure the result of a superficial heat treatment on metallic pieces, are destructive: a sample among these "identical" pieces is chosen, it is cut and then on its edge micro-hardness tests are performed (see Ref. [2]).

The same kind of destructive tests are often used to measure the residual stresses: the piece is cut in a special way in order to release some components of the stress tensor. Of course these methods have a great limitation. Some non destructive methods have been already proposed and are actually used: (i) the piece is deeply and plastically punched by spherical or pyramidal indenters (fitted hardness tests), (ii) the piece is auscultated by wave propagations (ultrasonic tests) or by X-rays. But with them, until now, the results are always incomplete.

The aim of this paper is to present a new "hardness" test. Indeed, we shall show that if there is no residual stress and if the structure is elastically homogeneous, the elastic limit at any point of this structure may be easily measured by a non-destructive method. This is based only on the Hertz theory of contact between two elastic bodies. The structure is, up to its elastic limit, successively "elastically" punched by spherical balls of different radius.

In order to make easy the proof of our affirmation, we shall first briefly recall the principles and limitations of classical hardness tests and the fundamental elements of Hertz theory of contact. We shall then describe the new "hardness" test with the automatic set-up and some of the data which allow its confirmation.

2. PRINCIPLES AND LIMITATIONS OF CLASSICAL HARDNESS TESTS

Classical hardness tests are based on an idealization of the real behaviour of metals. For a uniaxial loading of a specimen, one classically gets the stress-strain curve shown on Fig. 1. There are first the elastic behaviour, and when the load is increasing further the plastic behaviour. The real behaviour is very often idealized by a elastic perfect-plastic behaviour or even by a rigid perfect plastic behaviour (without hardening). The constitutive relations in the isotropic linear elastic domain are:

$$\epsilon_{ij} = -\frac{\nu}{E} (\sigma_{kk}) \delta_{ij} + \frac{(1+\nu)}{E} \sigma_{ij} \quad (1)$$

with: E , Young modulus; ν , Poisson ratio; ϵ_{ij} and σ_{ij} , components of the strain tensor (small strains) and of the stress tensor.

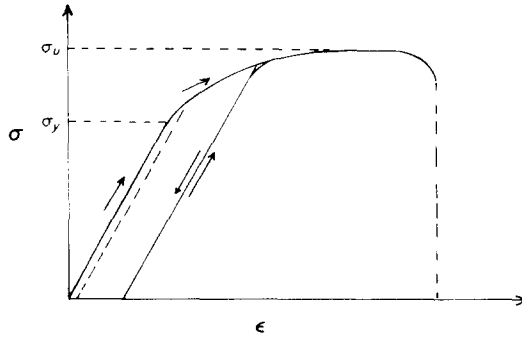


Fig. 1. Stress-strain curve.

The elastic domain is the domain where the criterion of plasticity

$$f(\sigma_{ij}) \leq 0 \tag{2}$$

is satisfied.

The Tresca's criterion:

$$\text{Sup}_{i,j} |\sigma_i - \sigma_j| - \sigma_y \leq 0, \tag{3}$$

and the Mises criterion:

$$(\sigma_1 - \sigma_2)^2 + (\sigma_2 - \sigma_3)^2 + (\sigma_3 - \sigma_1)^2 - 8\sigma_y^2 \leq 0, \tag{4}$$

(σ_i i = 1, 3, principal stresses; σ_y, elastic yield for a tensile test), are classically assumed for metals.

Hardness tests must be available to characterize the yield limit. These tests are based on the special case of the indentation of an homogeneous rigid perfect plastic semi-infinite body by a rigid flat indenter (Fig. 2).

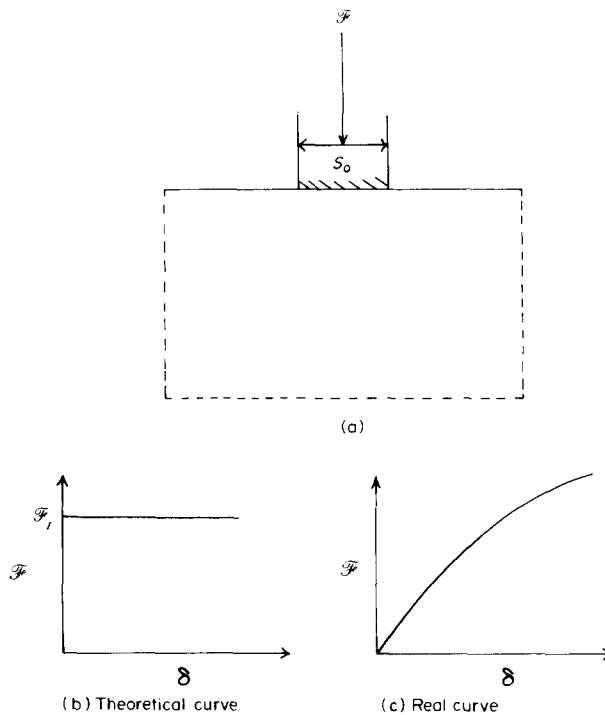


Fig. 2. Indentation of a thick plate by a flat indenter.

Theoretically the relation between the applied force on the indenter and its penetration inside the body is shown on Fig. 2(b): this force reaches a maximum \mathcal{F}_e ; it was proved that the mean pressure under the die is proportional to the yield limit σ :

$$P_e = \frac{\mathcal{F}_e}{S} = \alpha\sigma, \quad (\alpha \text{ constant}). \tag{5}$$

However experimentally on a real material the maximum force is very difficult to obtain: the real shape (Fig. 2c) results from the elasticity, the work hardening of the body and several other parameters. In the classical hardness tests (Brinell test, Vickers test, Rockwell test), the force is not measured; after a fixed load is applied, the hardness numbers are defined by the measurement of the prints leaved on the body.

Moreover only the surface may be tested. In order to know the internal mechanical characteristics it is generally necessary to cut the structure and on the edge to perform microhardness tests. For these reasons, we have tried to develop a test which allows the real yield limit to be measured, not only on the surface, but also inside the structure.

3. REVIEW OF SOME ELEMENTS OF THE HERTZ THEORY FOR ELASTIC CONTACT

Here, we shall only consider the elastic contact (without friction) of a spherical ball against a semi-infinite body which is bounded by a plane. It is well known that if (Fig. 3): E_1, ν_1 , are the

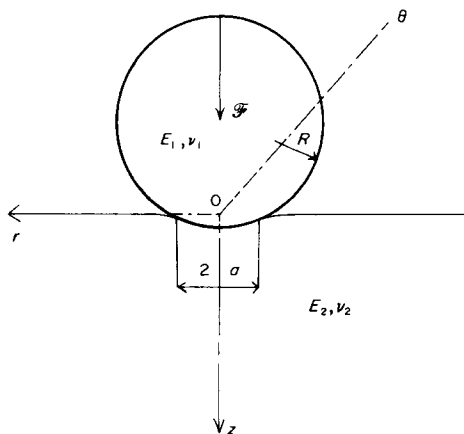


Fig. 3. Elastic contact sphere semi infinite body.

elastic constants for the die (Young's modulus and Poisson's ratio); E_2, ν_2 , the elastic constants for the body, R , is the radius of the ball, \mathcal{F} , the applied force on the ball, by putting:

$$\frac{1}{E} = \frac{1 - \nu_1^2}{E_1} + \frac{1 - \nu_2^2}{E_2} \tag{6}$$

(E is the equivalent modulus), then the radius of the area of contact a , and the maximal normal pressure are given by:

$$a = \sqrt[3]{\frac{3\mathcal{F}R}{4E}} \quad \sigma_0 = \frac{3\mathcal{F}}{2\pi a^2}. \tag{7}$$

If (O, r, θ, z) are the cylindrical coordinates where O is the center of the contact area, and Oz is the axis of symmetry directed inside the body, by using the transformation:

$$\begin{aligned} r &= a \operatorname{ch} \alpha \cos \beta & \alpha &\geq 0 \\ z &= a \operatorname{sh} \alpha \sin \beta & 0 &\leq \beta \leq \pi/2, \end{aligned} \tag{8}$$

it is also well known that the induced stress tensor in the body may be determined in an explicit form.

The non-zero components are equal to:

$$\begin{aligned} \frac{\sigma_{rr}}{\sigma_0} &= \text{sh } \alpha \sin \beta \left[(1 + \nu_2) \text{Arctg} \frac{1}{\text{sh } \alpha} - (1 - \nu_2) \frac{\text{sh } \alpha}{\text{ch}^2 \alpha} - \frac{\text{sh } \alpha \cos^2 \beta}{\text{ch}^2 \alpha (\text{sh}^2 \alpha + \sin^2 \beta)} \right] \\ &\quad - 2\nu_2 \sin \beta - \frac{1 - 2\nu_2}{3 \text{ch}^2 \alpha} \cdot \frac{2(1 + \sin \beta + \sin^2 \beta) - 3}{1 + \sin \beta} \\ \frac{\sigma_{\theta\theta}}{\sigma_0} &= \text{sh } \alpha \sin \beta \left[(1 + \nu_2) \text{Arctg} \frac{1}{\text{sh } \alpha} - (1 - \nu_2) \frac{\text{sh } \alpha}{\text{ch}^2 \alpha} \right] \\ &\quad - 2\nu_2 \sin \beta - \frac{1 - 2\nu_2}{3 \text{ch}^2 \alpha} \cdot \frac{1 + \sin \beta + \sin^2 \beta}{1 + \sin \beta} \\ \frac{\sigma_{zz}}{\sigma_0} &= \frac{-\sin^3 \beta}{\text{sh}^2 \alpha + \sin^2 \beta} \quad \frac{\sigma_{rz}}{\sigma_0} = \frac{-\text{sh } \alpha \cos \beta \sin^2 \beta}{\text{ch } \alpha (\text{sh}^2 \alpha + \sin^2 \beta)}. \end{aligned} \tag{9}$$

It is necessary to look at this stress tensor at some particular points: firstly on the axis of punching Oz : we have:

$$\begin{aligned} \sigma_{rr} = \sigma_{\theta\theta} &= \sigma_0 \left[(1 + \nu_2) \left(\frac{z}{a} \text{Arctg} \frac{a}{z} - 1 \right) + \frac{1}{2} \cdot \frac{a^2}{a^2 + z^2} \right] \\ \sigma_{zz} &= -\sigma_0 \frac{a^2}{a^2 + z^2} \end{aligned} \tag{10}$$

then on the surface of the body outside the area of contact ($r \geq a$), we get for the two non-zero components:

$$\sigma_{rr} = -\sigma_{\theta\theta} = \sigma_0 \frac{(1 - 2\nu_2)a^2}{3r^2} \equiv \frac{(1 - 2\nu_2)}{2\pi r^2} \mathcal{F}. \tag{11}$$

This is a pure shear stress state directly proportional to the applied force \mathcal{F} and independant of the radius of the ball.

If now, we study the criteria of plasticity for all the body, by assuming that there is no residual stress and taking either the Tresca criterion or the Mises one (expressions (3) or (4)), it is very easy to see that its maximum is reached on the axis Oz (Fig. 4) inside the body. Indeed, on this axis, these two criteria are identical to:

$$X_{\mathcal{F}}^R(z) \equiv \sigma_{rr}(z) - \sigma_{zz}(z). \tag{12}$$

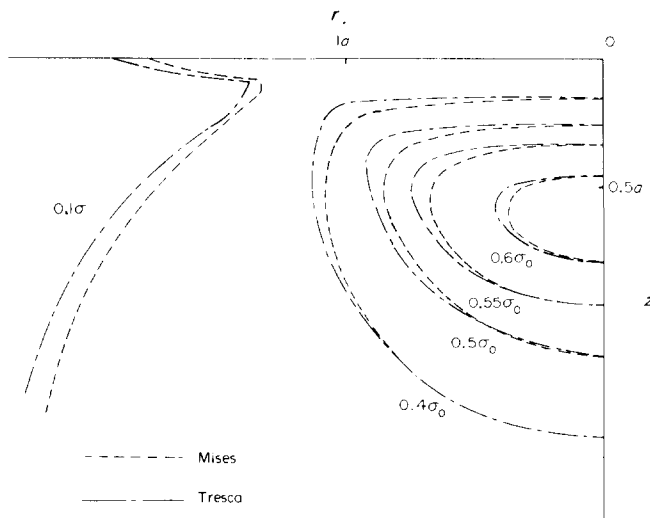


Fig. 4. Tresca and Mises criterions.

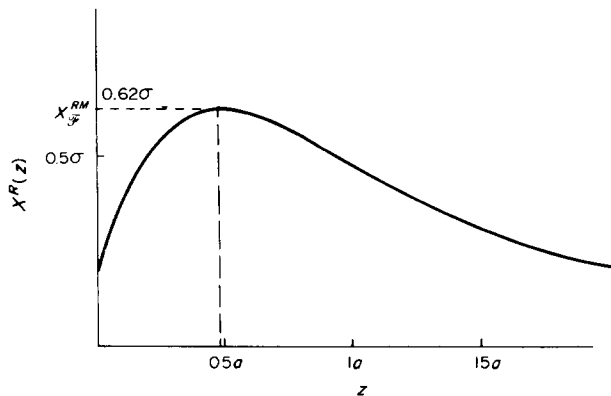


Fig. 5. Criterion on the punching axis.

This important quantity (Fig. 5) is always positive. The maximum of $X_{\mathcal{F}}^R$ is obtained for $(z/a) = \mu$ (with a Poisson ratio equal to 0.3, $\mu \approx 0.5$).

4. PRINCIPLES OF THE NEW "HARDNESS" TEST

Let us first come back to the true definition of the yield limit of the metallic bar (Fig. 1): it corresponds to the moment when the relation between the stress and the strain is no longer linear since some irreversible plastic strain appears.

Then, if now we want to measure the yield limit in *one* particular point of a body, we shall have: (i) to focus the "force", (ii) and to characterize the appearance of the plastic strain, precisely at *this* special point.

The spherical ball during the *elastic* punching of the body may be considered to be a "mechanical lens" as we can guess it by looking at the curves Fig. 4. However, in the general case where the yield limit in any point of the body is not at all known, the first point which will be plastified, when the applied force \mathcal{F} is increased further, cannot be *a priori* determined.

We are now able to describe the new test that we propose. We elastically punch the body by a spherical ball until a first plastic point appears; we repeat this operation with balls of different radius and in different points at the surface of the body. The compatibility of all these informations allows us to reach the elastic limit field inside the body.

It is very easy to see that there are two important problems in this new test: we have (i) to detect when there is a first plastic point inside the body, (ii) to know where this point is.

It is not possible to solve *explicitly* these problems for the general case. Here for simplicity we shall limit ourselves to the common example when the body is a rather thick plate which is elastically homogeneous and whose yield limit is only a function of the depth inside the body. This may result from a heat treatment at the surface of the plate. Since the body is a rather thick plate, the induced stress tensor during the elastic punching is approximately given by (9), (with (6)–(8)).

From the expressions of the stress tensor at the surface of the body and outside the contact area (11), we deduce that the strain tensor is reduced to:

$$\epsilon_{rr} = -\epsilon_{\theta\theta} = \frac{(1 - 2\nu_2)(1 + \nu_2)}{2\pi E_2} \frac{\mathcal{F}}{r^2}. \tag{13}$$

This means that the signal ϵ given by any strain gauge which is stuck outside the contact area, is directly proportional to the applied force \mathcal{F} and moreover that the slope \mathcal{F}/ϵ is independent of the radius R of the ball. *These properties are satisfied as long as there is purely elastic contact.*

Then, the force \mathcal{F} being increased further, when the relation between \mathcal{F} and ϵ is no more linear, necessarily there is a plastic point in the body (Fig. 6). \mathcal{F}_e^R is the elastic limit load for a special radius R . The first problem is thus solved.

By hypothesis, the yield limit is only a function of the depth; the curves, in Fig. 4, show thus that necessarily the first plastic point will be on the axis of symmetry Oz .

Let us first assume that we know the function $\sigma_y(z)$. When the contact is still purely elastic,

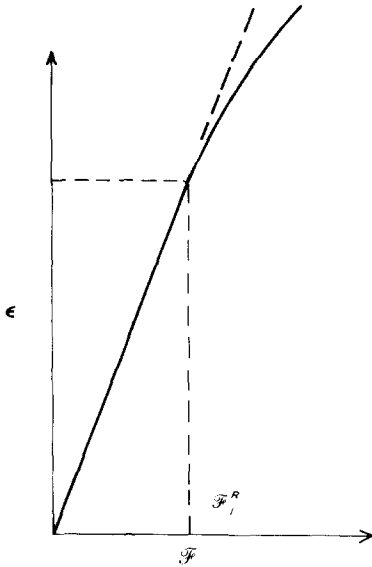


Fig. 6. Definition of \mathcal{F}_e^R .

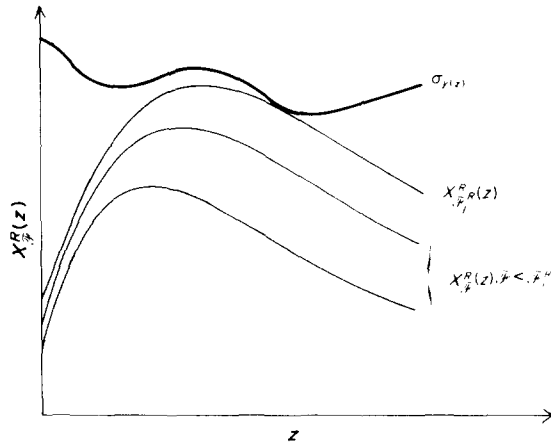


Fig. 7. Determination of the first plastic point for an increasing load.

the curve $X_{\mathcal{F}}^R(z)$ has no common point with $\sigma_y(z)$ (Fig. 7). On the contrary, for \mathcal{F}_e^R there is at least one common point between these two curves. If $\sigma_y(z)$ is a differentiable function the two curves must be tangent.

By writing this condition:

$$X_{\mathcal{F}_e^R}^R(z) = \sigma_y(z)$$

$$\frac{d}{dz} (X_{\mathcal{F}_e^R}^R(z) - \sigma_y(z)) = 0, \tag{16}$$

the first plastic point is exactly determined. In reality we have to determine the function $\sigma_y(z)$. Using only one elastic punch, with a ball of radius R , up to the elastic limit load \mathcal{F}_e^R , we may only say that necessarily the curve $\sigma_y(z)$ is above the curve $X_{\mathcal{F}_e^R}^R(z)$ and that there is at least one unknown common point.

If now we use balls of different radius R , by taking the envelope of the one parameter curves $X_{\mathcal{F}_e^R}^R(z)$, we easily obtain the function $\sigma_y(z)$. Our new Hardness test is thus really able to give a complete answer.

5. PRACTICAL SET UP AND EXPERIMENTAL CONFIRMATIONS

The experimental set-up which is necessary for this test is divided into two independent parts (Fig. 8). A frame permits the application of high loads. An hydraulic actuator with a simple pump is the most economical tool. At the extremity of the ram, it is possible to fix the indenter. The radius of the balls which are used to measure the yield limit up to about 5 mm in the depth of a steel plate, vary between ≈ 14 mm and 1200 mm. Of course, it is only necessary to use portion of the ball, (Fig. 9).

As we shall see it a little further, the elastic limit load, for these radii may reach values much greater than 100,000 N.

A cell gives an analogical signal which is proportional to the applied load \mathcal{F} .

The analogical output, ϵ , of a conditioner is proportional to the difference between the signals of two strain gauges which are stuck on the surface of the plate. We are using the actual special form of the strain tensor state $\epsilon_{rr} = +\epsilon/2$ and $\epsilon_{\theta\theta} = -\epsilon/2$, to eliminate a great part of the influence of any change in the room temperature during the test. This conditioner is the most important apparatus since the measured strain may be very small, sometimes only 10^{-6} .

For each radius of the indenter, during the test, the two analogical signals \mathcal{F} and ϵ are sent into a micro-computer through an analog-digital converter. This computer has two important functions: (i) It must detect the appearance of the first plastic point. The two signals \mathcal{F} , ϵ have to be compared until they are no longer proportional. Of course, since this limit is conventional, we must use a criterion.

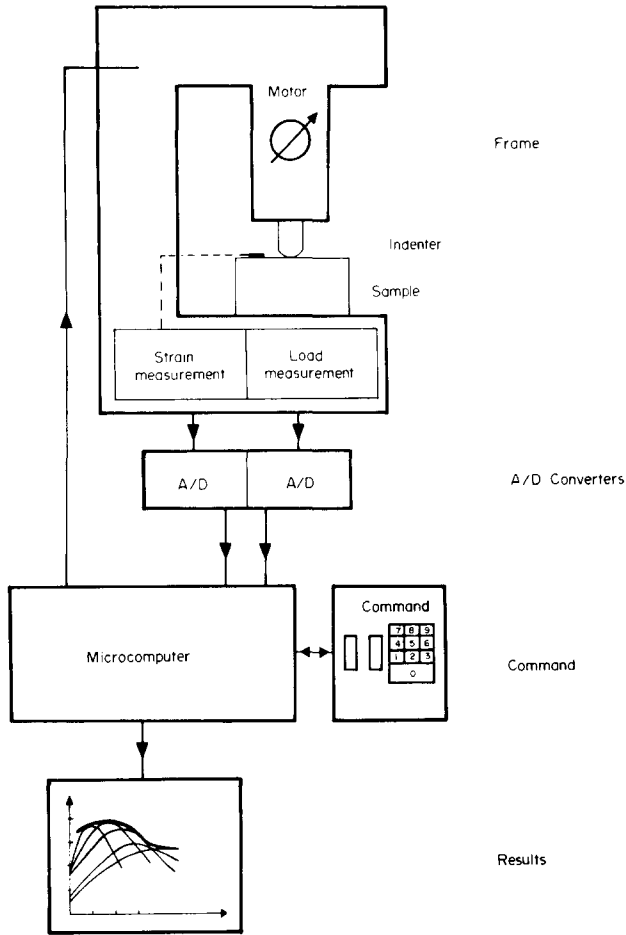


Fig. 8. Automatic set up.

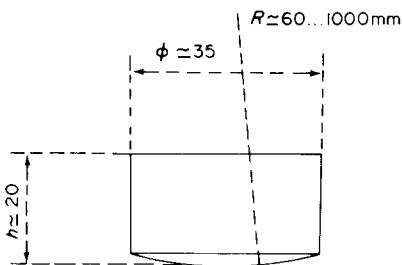


Fig. 9. Spherical dies.

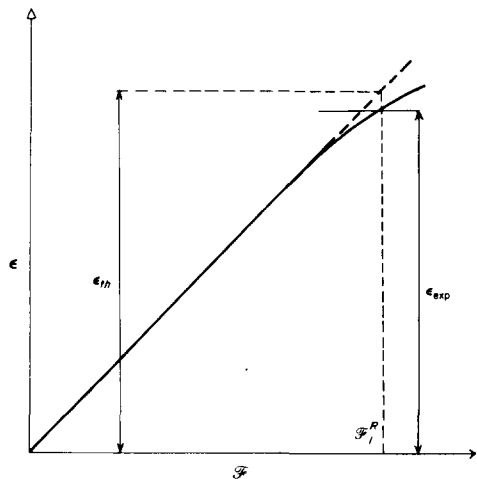


Fig. 10. Conventional definition of \mathcal{F}_e^R .

We found a very effective one (Fig. 10), which is based on the comparison between the measured strain ϵ_{exp} , and the "theoretical" strain ϵ_{th} (these two strains corresponds to the same load \mathcal{F}). Plasticity appears when:

$$\left| \frac{\epsilon_{th} - \epsilon_{exp}}{\epsilon_{th}} \right| = 1\%. \tag{15}$$

The computer must deal with signals which are perturbed by the usual noises. It then stops the

pump, keeps in this memories the pair of values (\mathcal{F}_e^R, R) and the elastic constants of the plate. (On the Fig. 11, one real experimental curve is shown). (ii) The second work of the computer is, eventually, to draw the curve $X_{\mathcal{F}_e^R}^R(z)$ on an appropriate plotter by using the formulae (12), (10), (7) and (6). Of course, the computer is only important in an automatic set-up. All the operations may be performed by hand as usual.

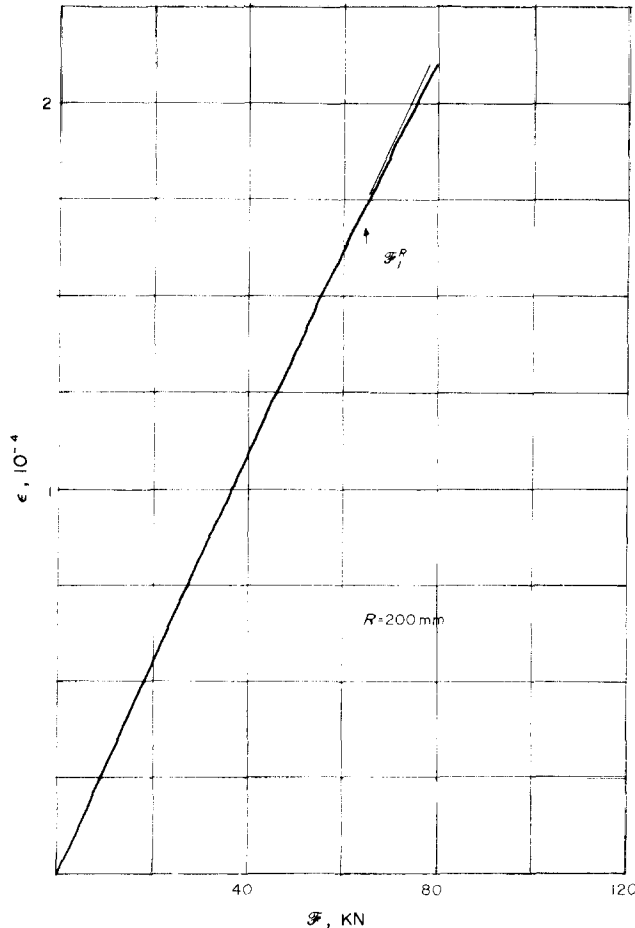


Fig. 11. Experimental curve.

Different indenters are successively fixed on the ram and the respective curves $X_{\mathcal{F}_e^R}^R(z)$ are all plotted on the same paper. The unknown yield limit function $\sigma_y(z)$, which is the envelope of these curves, is drawn by hand.

Several experiments have been performed to confirm this new "hardness" test. Here we only give two examples. We consider first a rather thick steel plate which has been annealed and which is thus elastically and plastically homogeneous. This is a cylindrical block of about 100 mm diameter and 80 mm high.

The pair of values obtained (\mathcal{F}_e^R, R) are given in the Table 1. The curves $X_{\mathcal{F}_e^R}^R(z)$ (Fig. 12) show that the envelope is a straight line and that we have almost the same yield limit σ_y (≈ 500 MPa) up to 5 mm depth in the plate.

By taking a small rod from this block and by applying the classical tensile test we found the same yield limit.

We consider this time, a cylinder which has been submitted to cementation on one of its ends. Due to the small sizes of the specimen ($\phi \approx 30$ mm and $h \approx 50$ mm) we could only use the balls with radius lower than 100 mm. (The radius of the contact area must be at least 10 times smaller than the minimum length of the body if we want to consider it as infinite). The new test gave the pair of values (\mathcal{F}_e^R, R) in Table 2 and the curves in Fig. 13.

Table 1.

R (mm)	60	100	150	200	300	400	600	800
\mathcal{F}_e^R (N)	700	1700	3750	6500	15,000	25,000	55,000	105,000

Table 2.

R (mm)	14	25.4	31.75	60	100
\mathcal{F}_e^R (N)	1700	6100	8500	15,000	30,000

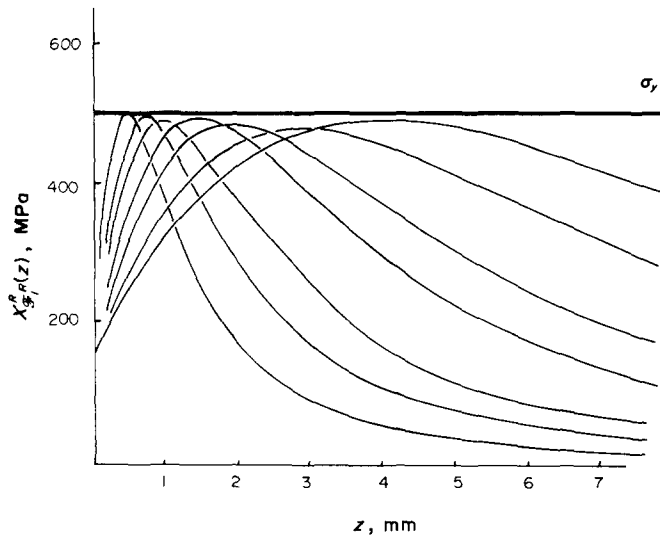


Fig. 12. Results on an homogeneous plate.

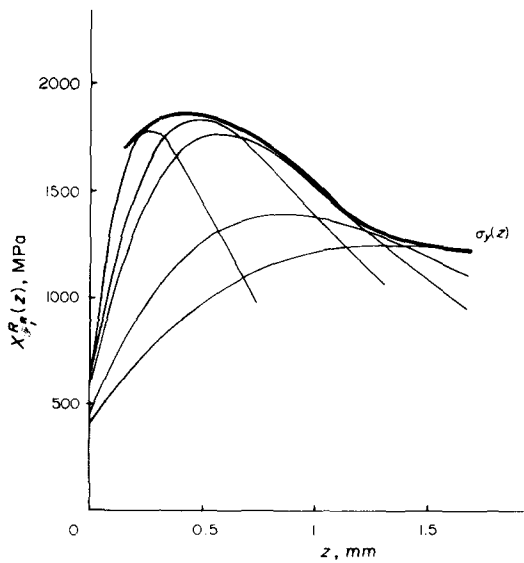


Fig. 13. Results on a cemented plate.

Then, we cut this sample and on its edge we applied classical microhardness Vickers tests. We exactly found the same depth of cementation (Fig. 14). Of course, there is no relation between the yield limit $\sigma_y(z)$ and the hardness number $HV(z)$; we may only look at the similarity of the curves.

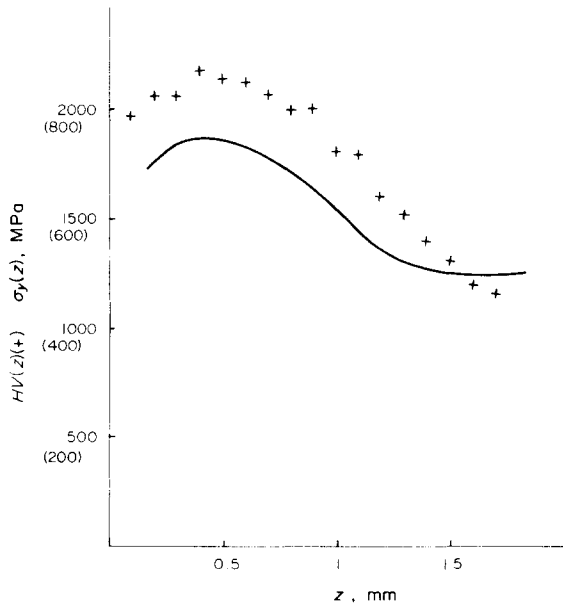


Fig. 14. Verification with classical destructive microhardness tests.

6. CONCLUSIONS

The new "hardness" test is very simple and automatically without any ambiguity provides us with a curve: the yield limit as a function of the depth in a flat body. Its generalization to a more complicated function of the yield limit or to a different shape of the body is rather straight-forward thanks to the micro-computer. However a special study has to be performed for each case. The automatic set-up will soon be marketed by the MAB Company, a member of the French SKF Group.

REFERENCES

1. J. F. Besseling, P. Van Bommel and S. Ten Hoeve, *Rapport ORE DT9* (1960).
2. R. Petty, hardness testing. *Technic of Metals Research. Measurement of Mechanical Properties*, Vol. 4, Part 2. Interscience, New York (1971).
3. M. R. Thomas and V. A. Hoerch, Stress due to the pressure of one elastic solid upon another. *Bull. 46*, Vol. XXXII. University of Illinois (1960).
4. J. Zarka, *Procédé de détermination de la limite élastique en profondeur*. Brevet (1973).
5. J. Zarka, *Procédé Non-Destructif de Détermination des Propriétés Mécaniques et des Contraintes dans une Pièce*. Brevet déposé par SKF et l'ANVAR 1974, (France, USA, URSS, Grande-Bretagne, Allemagne, Japon).